Design of an Ankle Rehabilitation Device Using Compliant Mechanisms

Citation: Sung, Edward, Alexander H. Slocum, Raymond Ma, Jonathan F. Bean, and Martin L. Culpepper. "Design of an Ankle Rehabilitation Device Using Compliant Mechanisms." Journal of Medical Devices 5, no. 1 (2011): 011001. © 2011 by ASME

As Published: http://dx.doi.org/10.1115/1.4002901

Publisher: ASME International

Persistent URL: http://hdl.handle.net/1721.1/120063

Version: Final published version: final published article, as it appeared in a journal, conference proceedings, or other formally published context

Design of an Ankle Rehabilitation Device Using Compliant Mechanisms

Edward Sung

Alexander H. Slocum, Jr.

Raymond Ma

Department of Mechanical Engineering,
Precision Compliant Systems Laboratory,
Massachusetts Institute of Technology,
Cambridge, MA 02139

Jonathan F. Bean
Harvard Medical School,
Department of Physical Medicine and Rehabilitation,
Spaulding Cambridge Outpatient Center,
Cambridge, MA 02138

Martin L. Culpepper
Department of Mechanical Engineering,
Precision Compliant Systems Laboratory,
Massachusetts Institute of Technology,
Cambridge, MA 02139

In this paper, we present the design, analysis, and testing of an ankle rehabilitation device (ARD), the purpose of which is to improve the efficacy of ankle joint complex (AJC) injury diagnosis and treatment. The ARD enables physicians to quantitatively measure the severity of an injury. This is done by measuring deficiencies in the joint's range of motion, as well as force, torque, and power output. Evaluation of the relative degree of recovery over time can also reduce the error associated with current methodologies for rehabilitation, which rely on measurements based on the patient's verbal response. A Wheatstone bridge circuit is used for the measurement of the various parameters as applied to the blades of complementary rotational flexures; the device is designed to measure motion about three axes of rotation in the ankle joint: pitch, roll, and yaw. A full bridge circuit is applied to each axis of rotation, and the use of multiple axes increases anatomically accurate measurement, enabling characterization of coupled motions. The device has flexibility and a range of motion such that it can be adjusted to take measurements of multiple different degrees of plantar or dorsiflexion of the AJC. The ARD is able to measure both range of motion, force, and torque output simultaneously. Experimental results show that there is significant coupled motion among the ankle joint rotations but that it is highly dependent on a subject's own physical development.
[DOI: 10.1115/1.4002901]

Keywords: ankle, rehabilitation, compliant mechanism

1 Introduction

The integrity of the human ankle joint complex (AJC) is critical for the prevention of injuries such as ankle sprains and strains. Injury to the AJC is one of the most common types of orthopedic injuries; current methods and devices for rehabilitation are varied in their efficacy. The clinical diagnosis and treatment of ankle injuries are largely dependent upon manual physical examination as well as the subjective assessment of a clinician [1]. Additionally, in older adults, neuromuscular impairments are recognized as important risk factors for fall related injuries because of their influence on balance and mobility [2].

There are few quantitative physical assessment tools that are readily available for implementation in clinical practice, which both specifically evaluate the performance of the AJC and are clinically reliable [3]. The development of an appropriate assessment tool is necessary to better quantify both the magnitude of neuromuscular deficit in the elderly and to monitor progress with different rehabilitative therapies among all patients with injuries to the AJC. Beyond reliability and validity, an ideal AJC assessment tool would be compact, portable, and simple to use in a variety of clinical settings. Furthermore, it would be able to test individuals in functional, weight-bearing positions that accurately represent the normal anatomical positions the joint would support.

Power output in the AJC has been shown to be correlated with functional capability [4]. A device that can accurately measure power and/or torque output in the ankle joint would potentially enable a more accurate diagnosis and lead to improvements in the efficacy of a rehabilitation regimen. Unfortunately, many quantitative measurement tools available and in use today do not have this capability. Noteworthy devices with quantitative diagnostic capabilities include hand-held dynamometers, isokinetic measures, gait pressure devices, and others such as the Rutgers ankle interface. These devices can be seen in Fig. 1 and Refs. [5–12], and Tables 1–4 show performance characteristics of each device.

2 Methods

A tool for the quantitative measurement of the AJC function has been developed in order to enable a more clinically ideal assessment of AJC performance. the ankle rehabilitation device (ARD) presented in this paper has the potential to enable physicians to obtain measurements of ankle joint performance (torque, force, power, and velocity) over positions within the joint's full range of motion (ROM).

2.1 Ankle Joint Complex Kinematics. The AJC has two subjoints—the true ankle joint and the subtalar joint, as can be seen in Fig. 2 [13]. The true ankle joint is located near the distal end of the fibula and is responsible for plantarflexion and dorsiflexion. The subtalar joint is located inferior to the true ankle joint and is responsible for inversion and eversion. Rotation in the ankle joint about the vertical axis is achieved through a combination of the motions of the two subjoints, as well as rotation of the tibia and fibula, also known as tibial/fibular rotation [14].

The ARD simulates the movement of the AJC by allowing rotation about the axes of the two subjoints, as well as tibial/fibular rotation. Because these joints are linked in series in the foot [14], the rotations of the ARD are designed to mimic this anatomical arrangement and thus are also linked in series. The inversion/eversion mechanism is coupled to the plantar/dorsiflexion mechanism, which in turn is connected to the ground.

2.1.1 Cartwheel Flexure Torque Sensor. The ARD uses cartwheel flexures as sensors to measure the deflection and load applied by the human ankle joint. Because ankle biomechanics vary significantly from patient to patient, the ARD is designed such that measurements are taken through rotation about the same three axes regardless of the location of the ankle joints. While there is potential for losses because of disparities in the coupling between

Manuscript received August 9, 2010; final manuscript received October 21, 2010; published online January 6, 2011. Assoc. Editor: Ted Conway.

Fig. 1 Gait pressure device (top left), [6] Rutgers ankle interface (top right), [8] hand-held dynamometer (bottom left), [10] and isokinetic dynamometer (bottom right) [12]

human and mechanical joint mechanics, the location of the mechanical joints are assumed to not be significantly relevant to measurement. This is a necessary design feature if the machine is to be compatible with a wide range of patient foot geometries [14].

Range of motion can be calculated based on measurements of the subject's foot correlated with rotation in the sensors. One axis of rotation simulates the true ankle joint and another simulates the subtalar joint; each allow for rotation of the respective ankle joints. Both axes are located about 3 in. (76 mm) from the average heel location both vertically and horizontally, as illustrated in Fig. 3. The lateral malleolus is used as a landmark for plantarflexion axis alignment. The cartwheel flexures are used to measure the output of the ankle joint around these axes of rotation.

The inner and outer rings of the cartwheel flexures are radially constrained and are connected by flexure blades that deflect as the two rotate in relation to each other, as shown in Fig. 4 [15].

Strain gauges are bonded to the surface of the flexure blades, and a full Wheatstone bridge circuit is used to measure strain. This allows for accurate measurement of the bending strain in the flexure blades. While the concept shown in Fig. 4 was used in the initial prototype, a new, nested cartwheel flexure was designed to rotate up to 2 deg, with an estimated maximum load of 250 in. lb (28.2 N m) in plantarflexion and 100 in. lb (11.3 N m) of torque in inversion.

The cartwheel flexures are calibrated before they are used to accurately measure force/torque, etc. This is done by recording the

Table 1 Gait pressure device characteristics

	Gait pressure device
Vendor	Zebris, Bertec, etc.
Usage	Measures foot-ground reaction forces and center of foot pressure during gait
Method	Measures gait pressure using multiple load cells placed in a treadmill [5]
Limitations	Cannot analyze the ROM of ankle joint [5] Cannot measure position or angular velocity of ankle rotation [5] High cost

Table 2 Rutgers ankle interface characteristics

	Rutgers ankle interface
Vendor	N/A
Usage	Personal device for in-home use. Move ankle joint through a range of motion and measure load capacity. A pseudo-passive Stewart Platform uses double-acting pneumatic cylinders to move the foot through a ROM
Method	and measure load-bearing capability [7].
Limitations	Low force output and input. Cannot exert larger forces on foot [7] and cannot support weight of patient [8]. Low reliability due to vibrations, large temperature fluctuations, and overheating of compressor [7]. High cost (projected).

Table 3 Hand-held dynamometer characteristics

	Hand-held dynamometer
Vendor	Hoggan, Jamar, etc.
Usage	Measure torque of joint to which device is held.
Method	Load cell, electric motor, etc.
Limitations	Variability between repeated measures [9] Variability between various dynamometers [9]

Table 4 Isokinetic dynamometer characteristics

	Isokinetic dynamometer
Vendor	Cybex, Biodex
Usage	Measure torque of joint during isolated movement
Method	Load cell, electric motor, etc.
Limitations	Variability between individual units [11] Large device, not mobile High cost

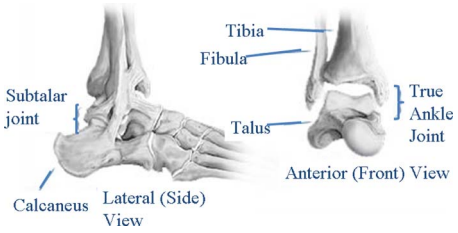

Fig. 2 Ankle joint complex [13]

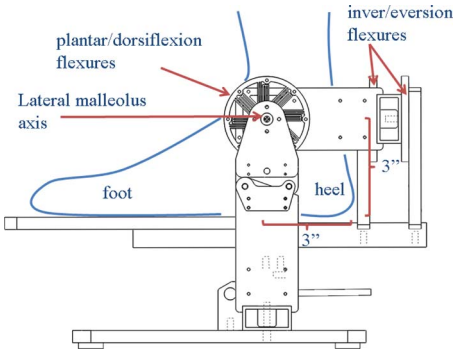

Fig. 3 Wire-frame solid model of prototype; the malleolus is aligned with the axis labeled in the figure as such

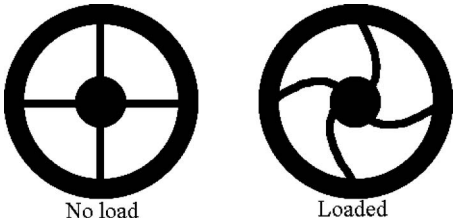

Fig. 4 Basic cartwheel flexure design [15]

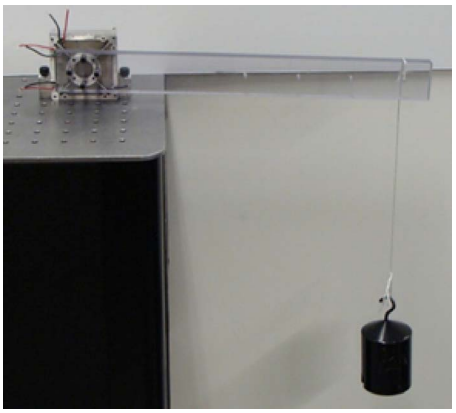

Fig. 5 Cartwheel flexure calibration setup

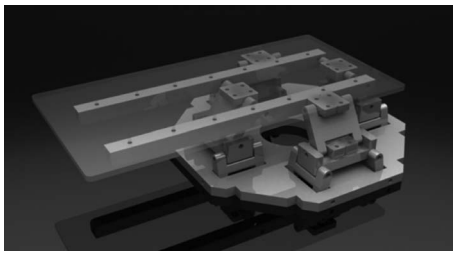

Fig. 6 Concept 1 solid model

relationship among torque, angular displacement, and output voltage in the calibration setup described by Ma [15], and shown in Fig. 5. The flexure is affixed to the ground, and weights of increasing mass are affixed to the lever arm to simulate increasing load. The measured response then yields a calibration constant that is used in further measurements to calculate load, torque, deflection, and power output.

After calibration, a measured torque and angular displacement can be differentiated to give angular velocity; power can be calculated by multiplication of torque and angular velocity. The cartwheel flexures used here are inherently superior for precision and accuracy because they significantly mitigate frictional and other losses, given that they operate within their elastic limits. Additionally, the Wheatstone bridge circuit ensures that the measurement will be less sensitive to temperature fluctuations [15].

2.2 Design Concepts and Concept Assessment. Multiple concepts were considered for this device initially, with previous iterations presented at the 2010 ASME medical devices conference [16]. The top two concepts considered are shown here. The device functional requirements and potential design parameters are presented first, and a weighted concept comparison chart is used to identify the best concept, as seen in Fig. 9.

2.2.1 Functional Requirements. The first step in the design process was to establish the functional requirements for the device; these can be seen in Table 5.

2.2.2 Concept 1. This design concept uses a nested 4 bar linkage mechanism to enable rotation about all three degrees of freedom in the human AJC. Rotation is about the instant centers of each set of linkages, and each nested linkage enables coupled motion about each axis of rotation. To accurately describe AJC movement, a 4 bar linkage would be stacked on top of another 4 bar linkage, orthogonal to the first linkage. Figure 6 shows a rendering of the concept solid model.

2.2.3 Concept 2. This design concept most accurately simulates ankle motion. Cartwheel flexures are used for torque and rotation sensing and are placed in series to ensure that they are subjected to the same forces. Coupled motion of the AJC is easily enabled and different foot anatomies can be accommodated with this design. A solid model of the three-axis rotation concept is seen in Fig. 7.

2.2.4 Concept Assessment: Pugh Chart. When a comparison of each concept to the desired device functional requirements is made, as seen in the weighted cost comparison chart shown in Fig. 8, concept 2 is the optimal design. Concept 1 is given a lower score for "AJC simulation" because the rotations generated using 4 bar linkages will also yield linear motion, which is undesirable in order to maintain anatomical accuracy of motion.

2.3 Modeling. The performance limit of a flexure is determined by the material's Young's modulus and yield stress. A low Young's modulus allows the flexure blades to deflect more readily, and yield stress determines how far the flexure blades can bend before failure. 7075-T6, an aluminum alloy commonly used in the fabrication of flexures [17], is used to manufacture cartwheel flexures for this device. Figure 9 shows the fatigue life for 7075-T6 aluminum. For testing purposes, a safety factor of 1.5 is assumed in order to maximize flexure rotation.

The basic cartwheel flexure, shown in Fig. 4, was utilized in the proof-of-concept device. This design failed during testing due to its low load capacity and range of motion. Increased rotation was achieved through the nested cartwheel flexure outlined by Ma et al. [18].

2.3.1 Flexure Beam Bending Calculations. Deformation of the flexure blades in the improved cartwheel flexure design is seen in Fig. 10. Deflection of the deformed flexure blade is given by the following equation, which is a modified version of the standard cantilevered beam bending equation,

$$\delta = \frac{2F\left(\frac{L}{2}\right)^3}{3EI}$$

For the cartwheel flexure designed for increased load capacity, the *plantarflexion flexure*, there are two blades in parallel attached to both the inner and outer hubs, and therefore $F_{applied} = F/2$. The modified displacement equation becomes

Table 5 Functional requirements for the ankle rehabilitation device

Functional requirement	Design parameters
1. Simulate AJC motions	Measure ankle output throughout the ROM of the ankle.
2. Rotation ~5 deg in both DOFs when foot position is set	Interface that does not give under load will stress the ankle joint and cause more pain than necessary.
3. Accommodate up to size 15 (U.S.) ft	The 99th percentile shoe length is 330 mm (13 in.). [17]
4. Support a load up to 200 lb	The maximum weight supported by each leg while testing.

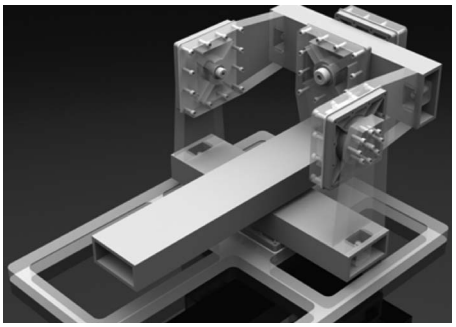

Fig. 7 Concept 2 solid model

$$\delta = \frac{2F\left(\frac{L_{\text{middle}}}{2}\right)^3}{3EI_{\text{middle}}} + 2\frac{\frac{F^3}{2\left(\frac{L_{\text{outer}}}{2}\right)}}{3EI_{\text{outer}}} = \frac{F}{12E\left(\frac{L_{\text{middle}}^3}{I_{\text{middle}}} + \frac{L_{\text{outer}}^3}{I_{\text{outer}}}\right)}$$

$$\delta = \frac{250\ \text{lbf}}{12 \times 104 \times 10^5\ \text{psi}}\left(\frac{(0.35\ \text{in.})^3}{4.5 \times 10^{-6}\ \text{in.}^4} + \frac{(0.4\ \text{in.})^3}{2.6 \times 10^{-6}\ \text{in.}^4}\right)$$

$$= 0.068\ \text{in. (1.7 mm)}$$

	Cost	Manufacturability	Data Interpretation	Flexure Motion Range	AJC Simulation	Score
Weight	2	1	3	2	3	N/A
4-Bar	3	2	2	1	2	22
3-Axis	2	1	3	3	3	29

Table 6: Pugh Chart for Concepts

Fig. 8 Pugh chart for concepts

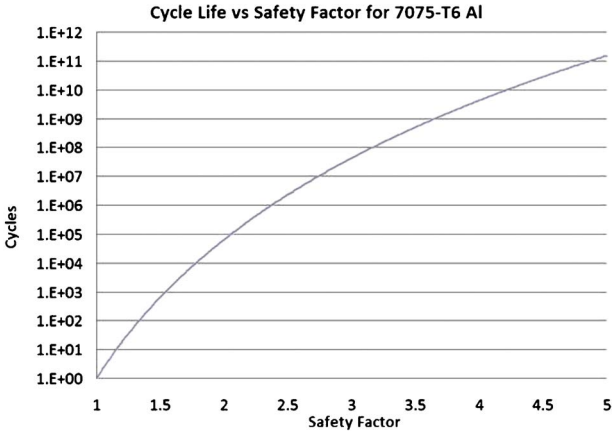

Fig. 9 Fatigue curve of 7075-T6 aluminum alloy

Fig. 10 Deformed flexure blade

As the radius of the flexure is 1.75 in. (44 mm), the flexure wheel is predicted to rotate 0.04 rad under the maximum load of 28.2 N m.

The cartwheel flexure designed for increased range of motion, the *inversion flexure*, the outer and inner blades are again in parallel. Thus, $F_{\text{applied to outer and inner blades}} = F/2$ again. The modified equation becomes

$$\delta = \frac{2I_{\text{outer}}}{100\ \text{lbf}}\left(\frac{(0.37\ \text{in.})^3}{2.6 \times 10^{-6}\ \text{in.}^4} + \frac{(0.50\ \text{in.})^3 + (0.30\ \text{in.})^3}{2 \times 5.63 \times 10^{-7}\ \text{in.}^4}\right) = 0.12\ \text{in. (3mm)}$$

As the radius of the flexure is 1.75 in. (44 mm), the flexure wheel is predicted to rotate 0.06 rad under the maximum load of 11.3 N m.

It should be noted that the difference between each flexure design is the result of interference between flexure blades. The blades of the plantarflexion flexure are thicker and thus can support increased load; however, if this beam geometry was used in the inversion flexure, the blades would contact each other under loading and lead to nonlinearity and parasitic errors during measurement. The modified geometry for the plantarflexion flexure accounts for this.

2.3.2 Finite Element Analysis. The finite element analysis of the flexure geometry is shown in Fig. 11; the plantarflexion and inversion flexures were both analyzed, and constraints and loads in each instance were accurately modeled. The inner "hub" was fixed, while load was applied to the outer hub. Both flexure designs resulted in improved performance over the initial cartwheel flexure design. Results of the FEA are shown in Table 6 and closely agree with the range of motion predicted by the closed-form analysis.

2.4 α-Prototype. Initially, flexures were implemented about all three axes of rotation. However, the vertical axis flexure assembly resulted in parasitic motions in the other two axes due to biomechanical compensation by the patient during testing. Because the vertical axis is not critical to the AJC kinematics, it was removed after preliminary testing in order to improve accuracy of measurement.

A second modification was made to enable diagnostics of the ankle at different angles in its ROM. A "pin-and-dial" angle adjustment mechanism was incorporated into the design to allow for positioning of the mechanism at different plantar/dorsiflexion angles. Shifting of the foot plate was now possible to discrete angles of 0.17 rad, 0.34 rad, and 0.52 rad in the plantarflexion direction.

There are three stages to the device. The base (first) stage is a 0.5 in. (12.7 mm) thick aluminum plate; the vertical bars that are fixed to the base support the lead screw angle adjustment mechanism, as seen in Fig. 12. They are also bolted to the inner ring of the plantarflexion flexures, as seen in Fig. 13. The second stage is mounted rigidly to the first using shoulder bolts. These allow the device to be weight-bearing and prevent parasitic loads from being applied in nonoptimal directions to the cartwheel flexure torque sensors.

The third stage is the foot plate. It connects to the second stage through the inversion flexures in a similar fashion. Finally, the foot is strapped in securely onto the foot plate using straps. Each flexure is part of a pair; specifically, there are two plantarflexion flexures and two inversion/eversion flexures. This allows for an increased number of strain gauges and increased accuracy of measurement [15].

After a design review of the prototype, it was decided that a continuous change in angle would be optimal over discrete changes in order to take full advantage of the device's capabilities.

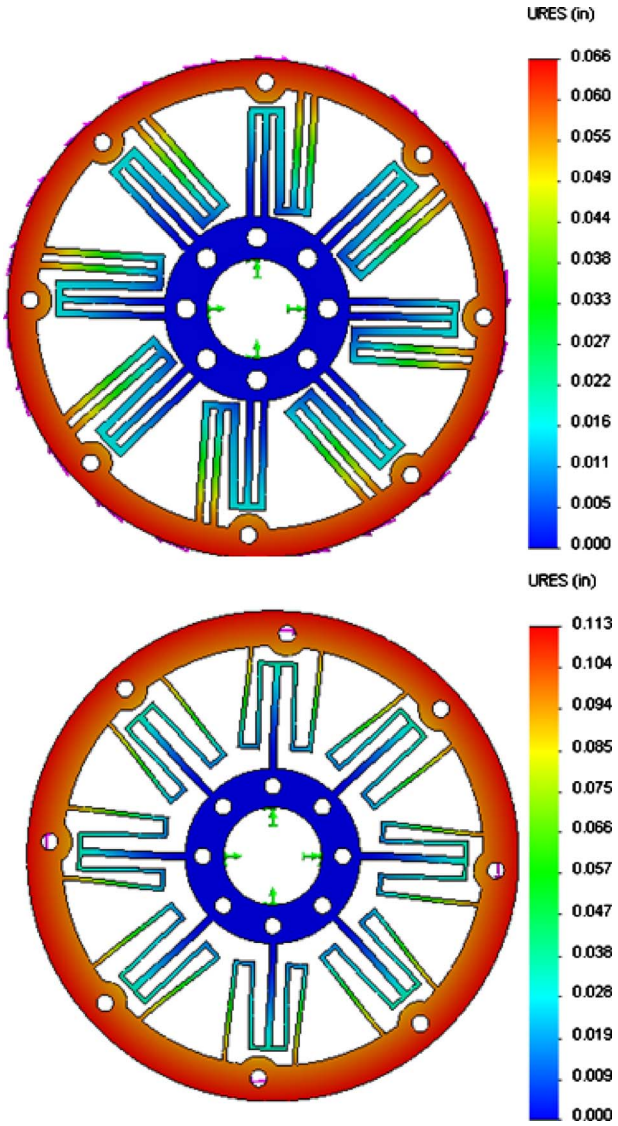

Fig. 11 Finite element analysis of plantar/dorsiflexion cartwheel flexure (top) and inversion/eversion cartwheel flexure (bottom)

A lead screw was introduced into the design to allow for continuous motion. Backlash was also considerably reduced with this addition, a solid model of which is shown in Fig. 12. The experimental prototype being used to measure ankle joint output can be seen in Fig. 14.

3 Experimental Results and Discussion

To use the ARD, a patient's foot must first be affixed to the device through straps attached to the device's foot plate, which would be performed under the supervision of a medical personnel. The patient's other foot must be free to move as necessary. It

Table 6 Flexure FEA results

Parameter	Plantarflexion flexure	Inversion flexure
Load	28.2 N m	11.3 N m
SF	1.5	1.5
Δangle	0.04 rad	0.06 rad

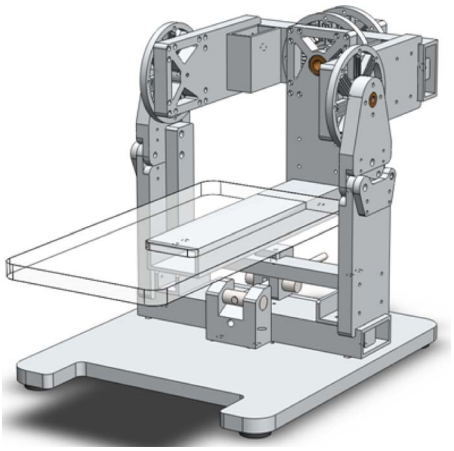

Fig. 12 Solid model of the α-prototype ankle rehabilitation device

should be noted that the ARD is a load-bearing machine and is capable of supporting patients weighing up to 180 kg.

Testing procedures would be implemented to establish a baseline and measure maximum torque output in plantarflexion, dorsiflexion, inversion, and eversion. To do this, the patient would be directed to apply as much force as possible in each direction of rotation. Measurement of power output is achieved through extraction of force and velocity data from the strain gauge measurement. Furthermore, current clinical tests for measurement of AJC health such as the unipedal stance (UST) and star-excursion balance test (SEBT) could be executed by the patient in the ARD. The quantitative characterization of the AJC capabilities using these tests would further improve physicians' abilities to diagnose and treat ankle injuries.

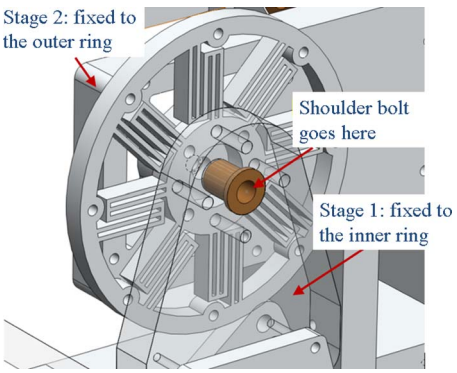

Fig. 13 Detail view of cartwheel flexure

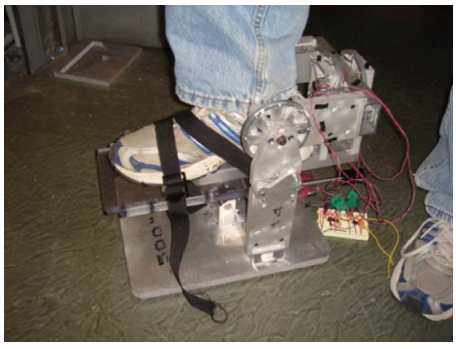

Fig. 14 Prototype ankle rehabilitation device in use. The patient's free foot is not in its normal position.

Table 7 Subject 1 (female, 47 kg) maximum torque

Mode	Plantar.	Dorsi.	Inver.	Ever.
Max plantar.	20.0	0	5.0	0
Max dorsi.	0	14.0	4.5	0
Max inver.	5.0	0	6.0	0
Max ever.	7.0	0	0	8.0

Improvements to the magnitude of the force and/or power output of the patient's ankle, along with reduced pain during testing, would be indicators as to the degree of ankle injury (if an initial visit) or the degree of ankle recovery (if a latter visit). Additionally, the rate of change in these parameters measured over multiple test subjects, each undergoing different rehabilitation routines or regimens, would help physicians to better determine which exercises are more efficacious for AJC rehabilitation.

Table 8 Subject 2 (male, 70 kg) maximum torque

Mode	Plantar.	Dorsi.	Inver.	Ever.
Max plantar.	42.0	0	4.0	0
Max dorsi.	0	19.0	0	2.5
Max inver.	7.5	0	12.0	0
Max ever.	4.5	0	0	9.0

Table 9 Subject 3 (male, 73 kg) maximum torque

Mode	Plantar.	Dorsi.	Inver.	Ever.
Max plantar.	36.9	0	3.5	0
Max dorsi.	0	28.0	0	3.1
Max inver.	25.0	0	12.0	0
Max ever.	23.0	0	0	12.5

Table 10 Subject 4 (male, 82 kg) maximum torque

Mode	Plantar.	Dorsi.	Inver.	Ever.
Max plantar.	47.0	0	3.1	0
Max dorsi.	0	36.9	7.5	0
Max inver.	6.0	0	12.0	0
Max ever.	5.0	0	0	10.1

Maximum torque output was measured for four test subjects in the four major directions—plantarflexion, dorsiflexion, inversion, and eversion. All testing was done with the foot in the horizontal position. The subjects were told to exert as much force as they could in each direction for 5 s. The results are shown in Tables 7–10. Figure 15 shows the coupled plantar/dorsiflexion motion exhibited by subject 1. Torque is in N m.

Because the two ankle subjoints are coupled, torque about one axis also causes torque to be applied about the other axis. For example, it can be seen that for all subjects, inversion and eversion motions also involved some plantarflexion. Inversion torque was limited to 12 N m, at which point the foot plate collided with the side of the structure. Therefore, it is expected that maximum torque values for inversion should be higher for subjects 2–4. This limitation in the design has been eliminated in time for the execution of a clinical trial utilizing this device.

When the subjects plantar flexed, some inversion was also observed. This suggests that when standing, more pressure is felt on the lateral part of the foot than the ball of the foot. It is possible that alterations in foot position or distance between the feet might have altered this pattern as well. Further study is warranted to investigate these effects.

Differences in individual ankle joint development can be seen as well from these data. Eversion by subject 1 is stronger than inversion. Conversely, inversion is stronger than eversion in the other subjects. In subject 3, inversion and eversion motions resulted in the subject also applying roughly double the torque in plantarflexion. The large coupled torque suggests that subject 3's ankle joint is less developed in the directions of inversion and eversion. Therefore, the ankle compensates and recruits muscles in largely the same motor pattern as seen in plantarflexion.

Subjects 2 and 3 show dorsiflexion coupling with eversion, while subjects 1 and 4 show dorsiflexion coupling with inversion. Plantarflexion did not show as much variation among the subjects. Therefore, it may be the case that dorsiflexion is much more subject to individual ankle development than plantarflexion.

It is usually expected that for internal rotation, plantarflexion is coupled with inversion, while for external rotation, dorsiflexion is coupled with eversion. However, these are not always the only observed modes of movement. An investigation conducted by Hicks [19] as cited by Glasoe et al. [20] showed primarily a cou-

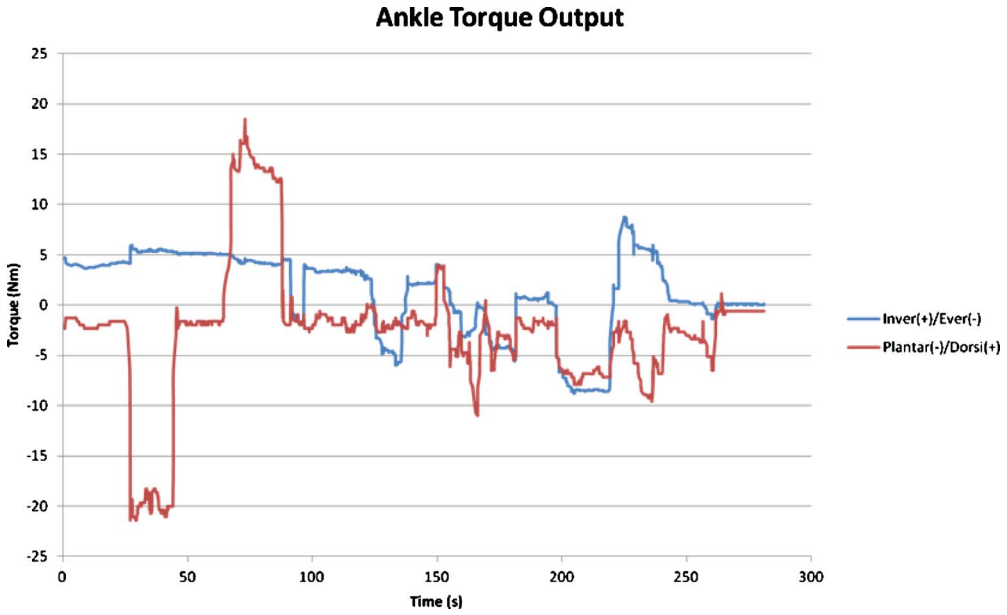

Fig. 15 Ankle joint torque output for subject 1

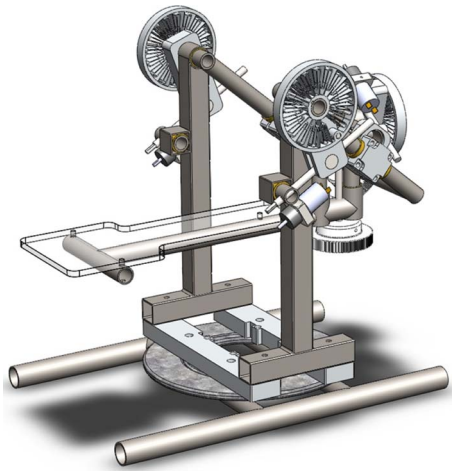

Fig. 16 Solid model of the beta-prototype design

pling of dorsiflexion with inversion and plantarflexion with eversion. Additionally, the experiments by Imhauser et al. [21] show a natural tendency in subjects to affect external rotation via coupling of plantarflexion and eversion. Therefore, it is expected that during further clinical validation of this device, both methods of coupling will be observed when a larger patient population is used.

4 Conclusions and Future Work

It has been shown that the ARD can measure torque output and also highlights the coupled motions of the human AJC. Further testing is needed to verify these conclusions. Additionally, the accuracy of the device must be compared against current schools of thought in ankle joint kinematics using existing technology such as force plates. Torque data from the ARD provide insight into how each subject's ankle has developed and moves and alone can be very beneficial in a clinical setting.

Preparations for a clinical validation of the device involving between 10 and 40 patients, each from two different age groups, are currently underway. Young patients, ages 18–40, and elderly patients, aged 65+, will be considered and about half of each patient group is expected to be composed of subjects with a history of chronic ankle injuries. This study will also be utilized to develop a clinically relevant testing protocol, with subsequent analysis across groups of varying age, injury status, and physical ability conducted after validation of the device's performance.

In addition to further study with the ankle rehabilitation device, there are several improvements to the current design that are being implemented:

1. *Angle adjustment mechanism*. The change in angle does not occur at the rotational axis as it should. This introduces a translation, and therefore misalignment, of the axes as the angle of the foot changes.
2. *Foot dimension adjustments*. While the average person wears a size 10 shoe, the average basketball player wears a size 14. The rotational axes of these two joints can be misaligned by as much as 2 in. Misalignment will introduce nonlinearity into the data and can put additional stress onto the ankle joint; as such an adjustment mechanism for each axis is being added.
3. *Varying flexure resistance*. The current device sandwiches the sensors between stages 1 and 2. Rapid removal or addition of additional flexures to change resistance and load capacity of the device is required.

A β-prototype solid model, shown in Fig. 16, includes adjustability for different foot geometries/sizes and also addresses the issues highlighted above. Foot dimensional adjustment is done through mechanisms that control vertical distances between the true ankle and subtalar joints and the vertical distance between the subtalar joint and the bottom of the patient's foot. Resistance and load capacity can be increased by simply adding additional cartwheel flexures.

Acknowledgment

The authors would like to thank Bill Buckley and the LMP shop for use of machine tools, Ken Stone and the MIT Hobby Shop for use of their waterjet, Jane Parish, Naoual Elasri, and Nicole Holt of Partners Healthcare for their assistance in procurement and organizing meetings, and Prof. Hughey and Prof. Lienhard for their help with designing the Wheatstone Bridge circuit.

References

[1] Griffin, L. Y., 2005, *Essentials of Musculoskeletal Care*, American Academy of Orthopaedic Surgeons, Brigham.
[2] Bean, J. F., Vora, A., and Frontera, W. R., 2004, "Benefits of Exercise for Community-Dwelling Older Adults," Arch. Phys. Med. Rehabil., **85**(3), pp. 31–42.
[3] Holmes, A., and Delahunt, E., 2009, "Treatment of Common Deficits Associated With Chronic Ankle Instability," Sports Med., **39**(3), pp. 207–224.
[4] Suzuki, T., Bean, J., and Fielding, R., 2001, "Muscle Power of the Ankle Flexors Predicts Functional Performance in Community-Dwelling Older Women," J. Am. Geriatr. Soc., **49**, pp. 1161–1167.
[5] Ranu, H. S., 1986, "Miniature Load Cells for the Measurement of Foot-Ground Reaction Forces and Centre of Foot Pressure During Gait," J. Biomed. Eng., **8**(2), pp. 175–177.
[6] http://www.noraxon.com/products/instruments/complete_gait_analysis.php
[7] Girone, M., Burdea, G., Bouzit, M., and Popescu, V. A., 2001, "Stewart Platform-Based System for Ankle Rehabilitation," Auton. Rob., **10**, pp. 203–212.
[8] Deutsch, J., Latonio, J., Burdea, G., and Boian, R., 2001, "Rehabilitation of Musculoskeletal Injuries Using the Rutgers Ankle Haptic Interface: Three Case Reports," Eurohaptics Conference, Birmingham UK, Jul. 1–4, pp. 6.
[9] Click, F. P., Bellew, J. W., Pitts, T., and Kay, R., 2003, "A Comparison of 3 Hand-Held Dynamometers Used to Measure Hip Abduction Strength," J. Strength Cond. Res., **17**(3), pp. 531–535.
[10] http://ajs.sagepub.com/content/34/3/370/F1.large.jpg
[11] Chow, J. W., 2001, "Isokinetic Exercises and Knee Joint Forces During Isokinetic Knee Extensions," University of Florida Department of Exercises and Sport Sciences 2001 Conference.
[12] http://www.health.uottawa.ca/biomech/images/biomech/kincom.jpg
[13] Patient Education, Foot and Ankle, http://www.orthoneuro1.com/patiented/ankle.php
[14] Arndt, A., Westblad, P., Winson, I., Hashimoto, T., and Lundberg, A., 2004, "Ankle and Subtalar Kinematics Measured With Intracortical Pins During the Stance Phase of Walking," Foot Ankle Int., **25**(5), pp. 357–364.
[15] Ma, R., Slocum, A. H., Jr., Sung, E., Bean, J. F., and Culpepper, M. L., 2010, "Torque Measurement via Compliant Mechanisms," ASME J. Mech. Rob., submitted.
[16] Ma, R., Slocum, A. H., Jr., Sung, E., Culpepper, M. L., and Bean, J. F., 2010, "Ankle-Rehabilitation via Compliant Mechanisms," Design of Medical Devices Conference, Minneapolis, MN, Apr. 13–15.
[17] Templer, J., 1992, *The Staircase: Studies of Hazards, Falls, and Safer Design*, MIT, Cambridge, MA.
[18] Choi, K. B., and Han, C. S., 2007, "Optimal Design of a Compliant Mechanism With Circular Notch Flexure Hinges," Proc. Inst. Mech. Eng., Part C: J. Mech. Eng. Sci., **221**(3), pp. 385–392.
[19] Hicks, J. H., 1953, "The Mechanics of the Foot, I: The Joints," J. Anat., **87**, pp. 345–357.
[20] Glasoe, W. M., Yack, H. J., and Saltzman, C. L., 1999,"Anatomy and Biomechanics of the First Ray," Phys. Ther., **79**(979), pp. 854–859.
[21] Imhauser, C. W., Siegler, S., Udupa, J. K., and Toy, J., 2008, "Subject-Specific Models Reveal the Existance of a Relationship Between Morphology of the Ankle Joint Complex and Its Passive Mechanical Properties," J. Biomech., **41**(6), pp. 1341–1349.